Supplemental material

Structure Based Design of Cyclically Permuted HIV-1 gp120 Trimers That Elicit Neutralizing Antibodies

Sannula Kesavardhana[‡], Raksha Das[‡], Michael Citron[§], Rohini Datta[‡], Linda Ecto[§], N. S. Srilatha[‡], Daniel DiStefano[§], Ryan Swoyer[§], Joseph G. Joyce[§], Somnath Dutta[‡], Celia C. LaBranche[¶], David C. Montefiori[¶], Jessica A. Flynn[§,1], and Raghavan Varadarajan[‡,1]

[‡]Molecular Biophysics Unit, Indian Institute of Science, Bangalore 560 012; [§]Merck Research Laboratories, West Point, PA 19486; and [¶]Department of Surgery, Duke University, Durham, North Carolina 27705

[1]To whom correspondence may be addressed. E-mail: varadar@mbu.iisc.ernet.in or jessica_flynn@merck.com

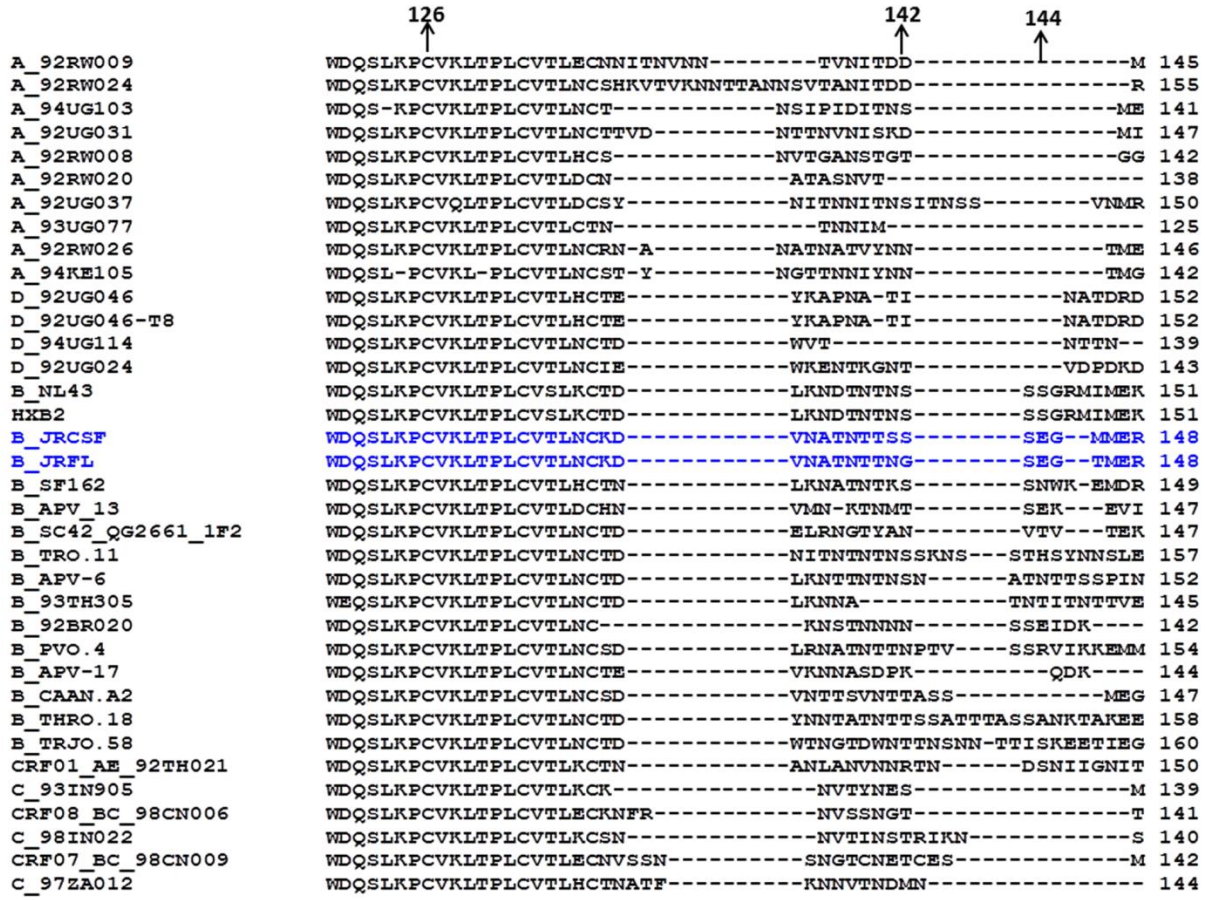
126
142
144
A_92RW009 WDQSLKPCVKLTPLCVTLECNNITNVNN--------TVNITDD---------M 145
A_92RW024 WDQSLKPCVKLTPLCVTLNCSHKVTVKNNTTANNSVTANITDD---------R 155
A_94UG103 WDQS-KPCVKLTPLCVTLNCT----------NSIPIDITNS---------ME 141
A_92UG031 WDQSLKPCVKLTPLCVTLNCTTVD---------NTTNVNISKD---------MI 147
A_92RW008 WDQSLKPCVKLTPLCVTLHCS----------NVTGANSTGT---------GG 142
A_92RW020 WDQSLKPCVKLTPLCVTLDCN----------ATASNVT---------- 138
A_92UG037 WDQSLKPCVQLTPLCVTLDCSY----------NITNNITNSITNSS--------VNMR 150
A_93UG077 WDQSLKPCVKLTPLCVTLCTN----------TNNIM---------- 125
A_92RW026 WDQSLKPCVKLTPLCVTLNCRN-A---------NATNATVYNN---------TME 146
A_94KE105 WDQSL-PCVKL-PLCVTLNCST-Y---------NGTTNNIYNN---------TMG 142
D_92UG046 WDQSLKPCVKLTPLCVTLHCTE----------YKAPNA-TI----------NATDRD 152
D_92UG046-T8 WDQSLKPCVKLTPLCVTLHCTE----------YKAPNA-TI----------NATDRD 152
D_94UG114 WDQSLKPCVKLTPLCVTLNCTD----------WVT---------NTTN-- 139
D_92UG024 WDQSLKPCVKLTPLCVTLNCIE----------WKENTKGNT----------VDPDKD 143
B_NL43 WDQSLKPCVKLTPLCVSLKCTD----------LKNDTNTNS--------SSGRMIMEK 151
HXB2 WDQSLKPCVKLTPLCVSLKCTD----------LKNDTNTNS--------SSGRMIMEK 151
B_JRCSF WDQSLKPCVKLTPLCVTLNCKD----------VNATNTTSS--------SEG--MMER 148
B_JRFL WDQSLKPCVKLTPLCVTLNCKD----------VNATNTTNG--------SEG--TMER 148
B_SF162 WDQSLKPCVKLTPLCVTLHCTN----------LKNATNTKS--------SNWK-EMDR 149
B_APV_13 WDQSLKPCVKLTPLCVTLDCHN----------VMN-KTNMT--------SEK---EVI 147
B_SC42_QG2661_1F2 WDQSLKPCVKLTPLCVTLNCTD----------ELRNGTYAN--------VTV---TEK 147
B_TRO.11 WDQSLKPCVKLTPLCVTLNCTD----------NITNTNTNSSKNS---STHSYNNSLE 157
B_APV-6 WDQSLKPCVKLTPLCVTLNCTD----------LKNTTNTNSN------ATNTTSSPIN 152
B_93TH305 WEQSLKPCVKLTPLCVTLNCTD----------LKNNA----------TNTITNTTVE 145
B_92BR020 WDQSLKPCVKLTPLCVTLNC----------KNSTNNNN-------SSEIDK---- 142
B_PVO.4 WDQSLKPCVKLTPLCVTLNCSD----------LRNATNTTNPTV----SSRVIKKEMM 154
B_APV-17 WDQSLKPCVKLTPLCVTLNCTE----------VKNNASDPK----------QDK---- 144
B_CAAN.A2 WDQSLKPCVKLTPLCVTLNCSD----------VNTTSVNTTASS----------MEG 147
B_THRO.18 WDQSLKPCVKLTPLCVTLNCTD----------YNNTATNTTSSATTTASSANKTAKEE 158
B_TRJO.58 WDQSLKPCVKLTPLCVTLNCTD----------WTNGTDWNTTNSNN-TTISKEETIEG 160
CRF01_AE_92TH021 WDQSLKPCVKLTPLCVTLKCTN----------ANLANVNNRTN------DSNIIGNIT 150
C_93IN905 WDQSLKPCVKLTPLCVTLKCK----------NVTYNES----------M 139
CRF08_BC_98CN006 WDQSLKPCVKLTPLCVTLECKNFR----------NVSSNGT----------T 141
C_98IN022 WDQSLKPCVKLTPLCVTLKCSN----------NVTINSTRIKN----------S 140
CRF07_BC_98CN009 WDQSLKPCVKLTPLCVTLECNVSSN----------SNGTCNETCES----------M 142
C_97ZA012 WDQSLKPCVKLTPLCVTLHCTNATF----------KNNVTNDMN---------- 144
185
186
196
A_92RW009 KGEKNCSFNMTTELRDKKQRVYSLFYRLDIVQINSNSNNSSHNQ------YRLINCNTSA 199
A_92RW024 EDLKNCSFNTTTEIRDKKQKVYSLFYKLDVVPIG---DNNSSNE------YRLINCNTSA 206
A_94UG103 -EIKNCSY----------NNSSSNSE------YRLINCNTSA 166
A_92UG031 GEIKNCSYNMTTELRDKKQKIYSLFYRLDVVPINESNSSDNFSE------YRLINCNTSA 201
A_92RW008 EEIKNCSYNITTELRDKRKKVYSLFYRLDIVQLS--SNNSNSNE------YRLINCNTSA 194
A_92RW020 NEMRNCSFNITTELKDKKQQVYSLFYKLDVVQIN---EKNETDK------YRLINCNTSA 189
A_92UG037 EEIKNCSFNMTTELRDKNRKVYSLFYKLDVVQINN--GNNSSNL------YRLINCNTSA 202
A_93UG077 -EIKNCSFNMTTELRDQ--KVYSLFR-LDVVQIE-----SDSNR------YRLINCNTSA 170
A_92RW026 GEIKNCSFNITTELRDKTRKEHALFYRLDIVPLNEGNSNSTENSS----DYRLINCNTSA 202
A_94KE105 DEIKNCSF-MTTEVRDKSKKVHALFYKLDIVPLNDSVDESNRN-------YRLINCNTSA 194
D_92UG046 IGMKNCSFNVTTEVINKKKQEHALFYKLDVVQMDDNSTN---------TNYRLINCNTSV 203
D_92UG046-T8 IGMKNCSFNVTTEVINKKKQEHALFYKLDVVQMDDNSTN---------TNYRLINCNTSV 203
D_94UG114 -TMTNCSFNITTEIRDKKKQVQALFYKLDVVKINDTDSND--------TSYRLINCNTSA 190
D_92UG024 IGMKNCSFNVTTER--KKKQVYALFYKLDVVQMND-NTN---------TSYRLINCNTSA 191
B_NL43 GEIKNCSFNISTSIRDKVQKEYAFFYKLDIVPIDN------------TSYRLISCNTSV 198
HXB2 GEIKNCSFNISTSIRGKVQKEYAFFYKLDIIPIDN-----------DTTSYKLTSCNTSV 200
B_JRCSF GEIKNCSFNITKSIRNKVQKEYALFYKLDVVPIDNK----------NNTKYRLISCNTSV 198
B_JRFL GEIKNCSFNITTSIRDEVQKEYALFYKLDVVPIDN-----------NNTSYRLISCDTSV 197
B_SF162 GEIKNCSFKVTTSIRNKMQKEYALFYKLDVVPIDN-----------DNTSYKLINCNTSV 198
B_APV_13 GEMKNCSFNVTTNIRDKVKSEYALFYKLDIVQIKEDGSNTS---------YRLTSCNTSV 198
B_SC42_QG2661_1F2 GEIKNCSFNITTAIRDKVQKTYALFYRLDVVPIDNNHGNSSS----NYSNYRLINCNTSV 203
B_TRO.11 GEMKNCSFNITAGIRDKVKKEYALFYKLDVVPIEEDKDT-------NKTTYRLRSCNTSV 210
B_APV-6 GEMKNCSFNITSTIRNKMHKEYALLYKLDIVPIDGDN-----------TTYTLTNCNTSV 201
B_93TH305 GEMKNCSFNITTSIREKVKREYALFYRLDVVPINDDNN--------NDTSYRLISCNTSV 197
B_92BR020 GEIKNCSFTTS---VDKVKKEYALFYNLDVVQINDN-------------SYRLTSCNTSV 186
B_PVO.4 GEVKNCSFNVTTDIRDRMQKVYALFYRPDVVPIQDHTIENNNTI-ENNTTYRLISCNTSV 213
B_APV-17 -EVTNCSFNITTSIRDKVQKEYAIFYKYDVVPIDDSDNNSTN------TSYRLISCNTSV 197
B_CAAN.A2 GEIKNCSFNTTTSMSDKMQKEYALFYTLDVVPIVKEN-----------NTYRLISCNTSV 196
B_THRO.18 AVMKNCSFNITTNVRDKVKREYALFYNLDVVKLEEGE-----------TSYRLVSCNTSV 207
B_TRJO.58 GEMKNCSFNITTATGDKK-KERAFFYKLDVAPIDNSN-----------TSYRLISCNTSV 208
CRF01_AE_92TH021 DEIRNCSFNMTTEIRDRKQKVHALFYKLDIVQIEDDKNSS--------EEYRLINCNTSV 202
C_93IN905 QEIKNCSFNATTDLRDRKQTVQALFYKLDIVSLNEK-NSSE--------YYRLINCNTSA 190
CRF08_BC_98CN006 NEEIKCSFNTT--LRDKEKKVSALFYRLDIVPLNDK-NSSESGK-NSSEYYRLINCNTSA 197
C_98IN022 EEIKNCSFNTTT-ELDRRKKEYALFYRLDITPLDNKKNSSE----NSSEYYRLINCNTSA 195
CRF07_BC_98CN009 KEMKNCSFNATT---VDKQTVYALFYRLDIVPLKNSSNSS----------YRLINCNTSA 189
C_97ZA012 KEIRNCSFNTTTEIRDKKQQGYALFYRPDIVLLKENRNNSN------NSEYILINCNAST 198

Figure S1: Sequence alignment of HIV-1 gp120 V1V2 loop region from various HIV-1 subtypes. V1V2 loop region is variable in sequence identity and length across different subtypes of HIV-1. The sequence information from various subtypes of HIV-1 suggests that V1 and V2 loop regions can tolerate mutations and insertions. The residues where gp120 was cyclically permuted to make trimers are marked. The JRFL and JRCSF sequences which were used for making cyclic permutants are highlighted in blue.

1 JRFL gp120

EVVLENVTEHFNMWKNNMVEQMQEDIISLWDQSLKPCVKLTPLCVTLNCKDVNATNTTNDSE
GTMERGEIKNCSFNITTSIRDKVQKEYALFYKLDVVPIDNNNTSYRLISCDTSVITQACPKI
SFEPIPIHYCAPAGFAILKCNDKTFNGKGPCKNVSTVQCTHGIRPVVSTQLLLNGSLAEEEV
VIRSDNFTNNAKTIIVQLKESVEINCTRPNNNTRKSIHIGPGRAFYTTGEIIGDIRQAHCNI
SRAKWNDTLKQIVIKLREQFENKTIVFNHSSGGDPEIVMHSFNCGGEFFYCNSTQLFNSTWN
NNTEGSNNTEGNTITLPCRIKQIINMWQEVGKAMYAPPIRGQIRCSSNITGLLLTRDGGINE
NGTEIFRPGGGDMRDNWRSELYKYKVVKIEPLGVAPTKAKRRVVQREKR

2 JRFL-hCMP-V1cyc

EEDPCACESLVKFQAKVEGLLQALTRKLEAVSKRLAILENTVVRSEGTMERGEIEISKNCSF
NITTSIRDEVQKEYALFYKLDVVPIDNNNTSYRLISCDTSVITQACPKISFEPIPIHYCAPA
GFAILKCNDKTFNGKGPCKNVSTVQCTHGIRPVVSTQLLLNGSLAEEEVVIRSDNFTNNAKT
IIVQLKESVEINCTRPNNNTRKSIHIGPGRAFYTTGEIIGDIRQAHCNISRAKWNDTLKQIV
IKLREQFENKTIVFNHSSGGDPEIVMHSFNCGGEFFYCNSTQLFNSTWNNNTEGSNNTEGNT
ITLPCRIKQIINMWQEVGKAMYAPPIRGQIRCSSNITGLLLTRDGGINENGTEIFRPGGGDM
RDNWRSELYKYKVVKIEPLGVAPTKAKRRVVQREKRGSAGSAGSSRSAGSAGSAGSEVVLEN
VTEHFNMWKNNMVEQMQEDIISLWDQSLKPCVKLTPLCVTLNCKDVNATNTTND

3 JRCSF-hCMP-V1cyc

EEDPCACESLVKFQAKVEGLLQALTRKLEAVSKRLAILENTVVASEGMMERGEIKNCSFNIT
KSIRNKVQKEYALFYKLDVVPIDNKNNTKYRLISCNTSVITQACPKVSFEPIPIHYCAPAGF
AILKCNNKTFNGKGQCKNVSTVQCTHGIRPVVSTQLLLNGSLAEEKVVIRSDNFTDNAKTII
VQLNESVKINCTRPSNNTRKSIHIGPGRAFYTTGEIIGDIRQAHCNISRAQWNNTLKQIVEK
LREQFNNKTIVFTHSSGGDPEIVMHSFNCGGEFFYCNSTQLFNSTWNDTEKSSGTEGNDTII
LPCRIKQIINMWQEVGKAMYAPPIKGQIRCSSNITGLLLTRDGGKNESEIEIFRPGGGDMRD
NWRSELYKYKVVKIEPLGVAPTKAKRRVVQREKRGSAGSAGSSRSAGSAGSAGSEVVLENVT
EDFNMWKNNMVEQMQEDVINLWDQSLKPCVKLTPLCVTLNCKDVNATNTTS

4 JRFLgp120-L6-hCMP

EVVLENVTEHFNMWKNNMVEQMQEDIISLWDQSLKPCVKLTPLCVTLNCKDVNATNTTNDSE
GTMERGEIKNCSFNITTSIRDKVQKEYALFYKLDVVPIDNNNTSYRLISCDTSVITQACPKI
SFEPIPIHYCAPAGFAILKCNDKTFNGKGPCKNVSTVQCTHGIRPVVSTQLLLNGSLAEEEV
VIRSDNFTNNAKTIIVQLKESVEINCTRPNNNTRKSIHIGPGRAFYTTGEIIGDIRQAHCNI
SRAKWNDTLKQIVIKLREQFENKTIVFNHSSGGDPEIVMHSFNCGGEFFYCNSTQLFNSTWN
NNTEGSNNTEGNTITLPCRIKQIINMWQEVGKAMYAPPIRGQIRCSSNITGLLLTRDGGINE
NGTEIFRPGGGDMRDNWRSELYKYKVVKIEPLGVAPTKAKRRVVQREKRASGSAGSAGSEED
PCACESLVKFQAKVEGLLQALTRKLEAVSKRLAILENTVV

Figure S2: Amino acid sequences of JRFL gp120, JRFL-hCMP-V1cyc, JRCSF-hCMP-V1cyc and JRFLgp120-L6-hCMP immunogens characterized in this study. The sequence of the hCMP trimerization domain is in green, the sequence of flexible soluble linkers is in red and the extra amino acid residues in the sequence which are encoded by restriction site nucleotide sequence is in blue. All the sequences were based on JRFL gp120 amino acid sequence except JRCSF-hCMP-V1cyc, which is based on JRCSF gp120 sequence. The JRFL-hCMP-V1cyc and JRCSF-hCMP-V1cyc immunogens show 95% similarity and 91% identity with each other in their amino acid sequence. The genes coding for these protein sequences were human codon optimized.

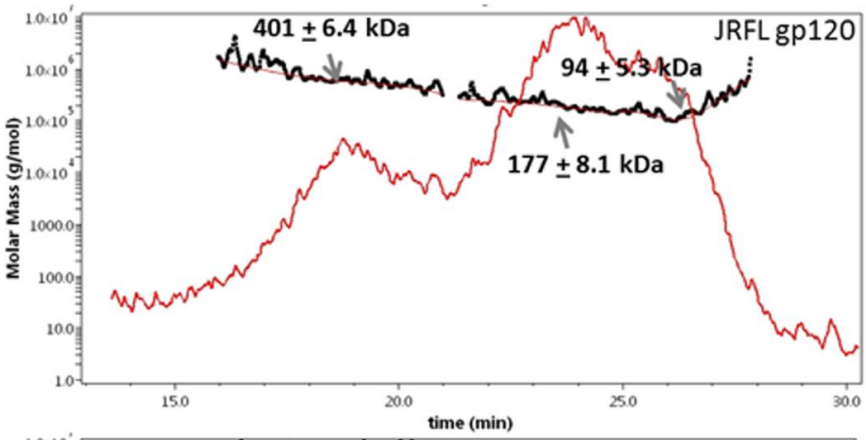
JRFL gp120
401 ± 6.4 kDa
94 ± 5.3 kDa
177 ± 8.1 kDa
Molar Mass (g/mol)
time (min)

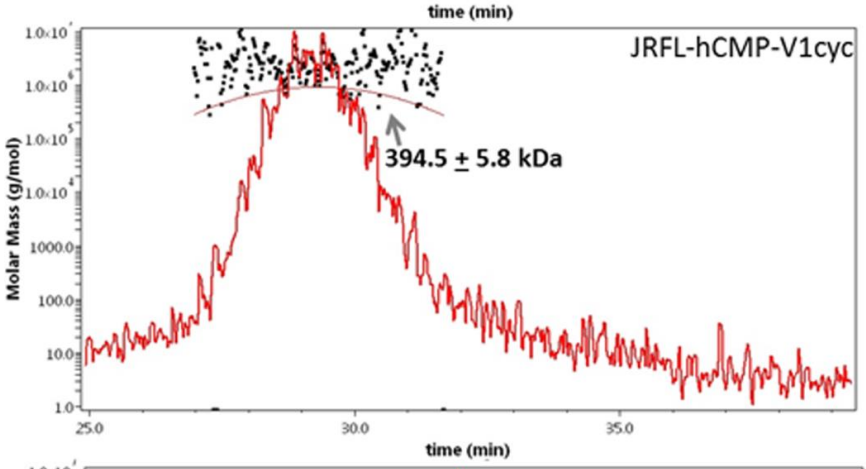
JRFL-hCMP-V1cyc
394.5 ± 5.8 kDa
Molar Mass (g/mol)
time (min)

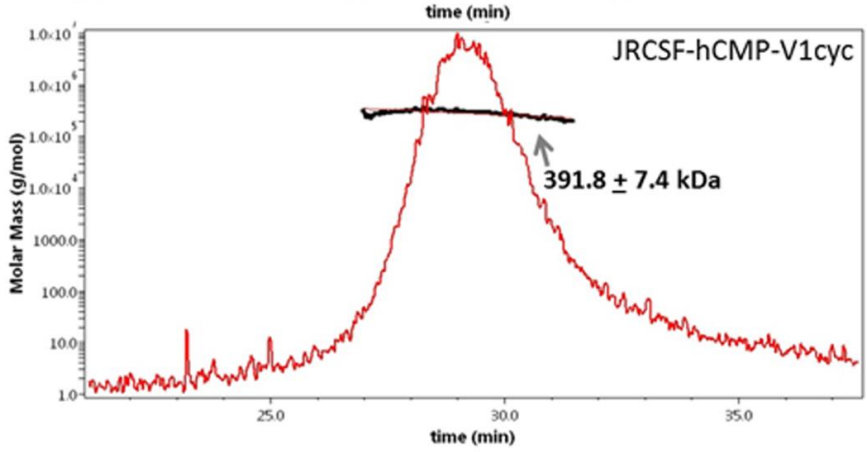
JRCSF-hCMP-V1cyc
391.8 ± 7.4 kDa
Molar Mass (g/mol)
time (min)

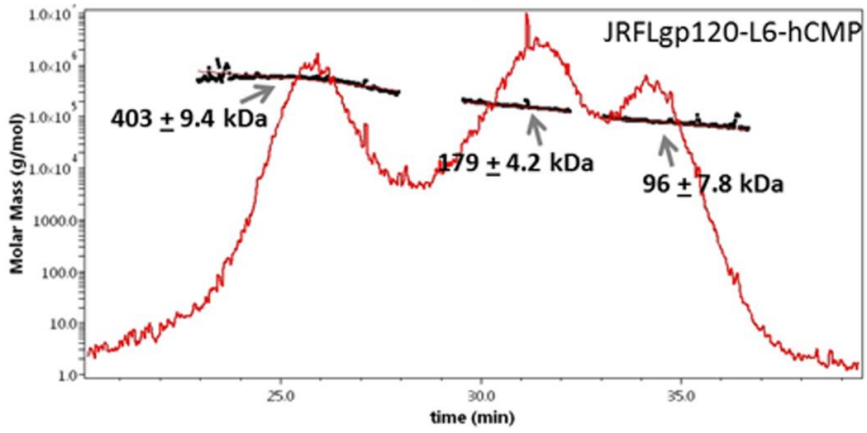
JRFLgp120-L6-hCMP
403 ± 9.4 kDa
179 ± 4.2 kDa
96 ± 7.8 kDa
Molar Mass (g/mol)
time (min)

Figure S3: Analysis of purified, soluble JRFL gp120, JRFL-hCMP-V1cyc, JRCSF-hCMP-V1cyc and JRFLgp120-L6-hCMP in PBS buffer, pH 7.4 at 25°C by SEC-MALS. Proteins were analyzed using a Superdex-200 analytical gel filtration column connected to UV, MALS (miniDAWN TREOS) and refractive index (Waters) detectors for molecular mass determination. Traces for light scattering from SEC-MALS are represented in red. The fitted areas in elution peaks are represented in black dots with a red line across the elution peaks. The average molecular masses for each elution peak are indicated.

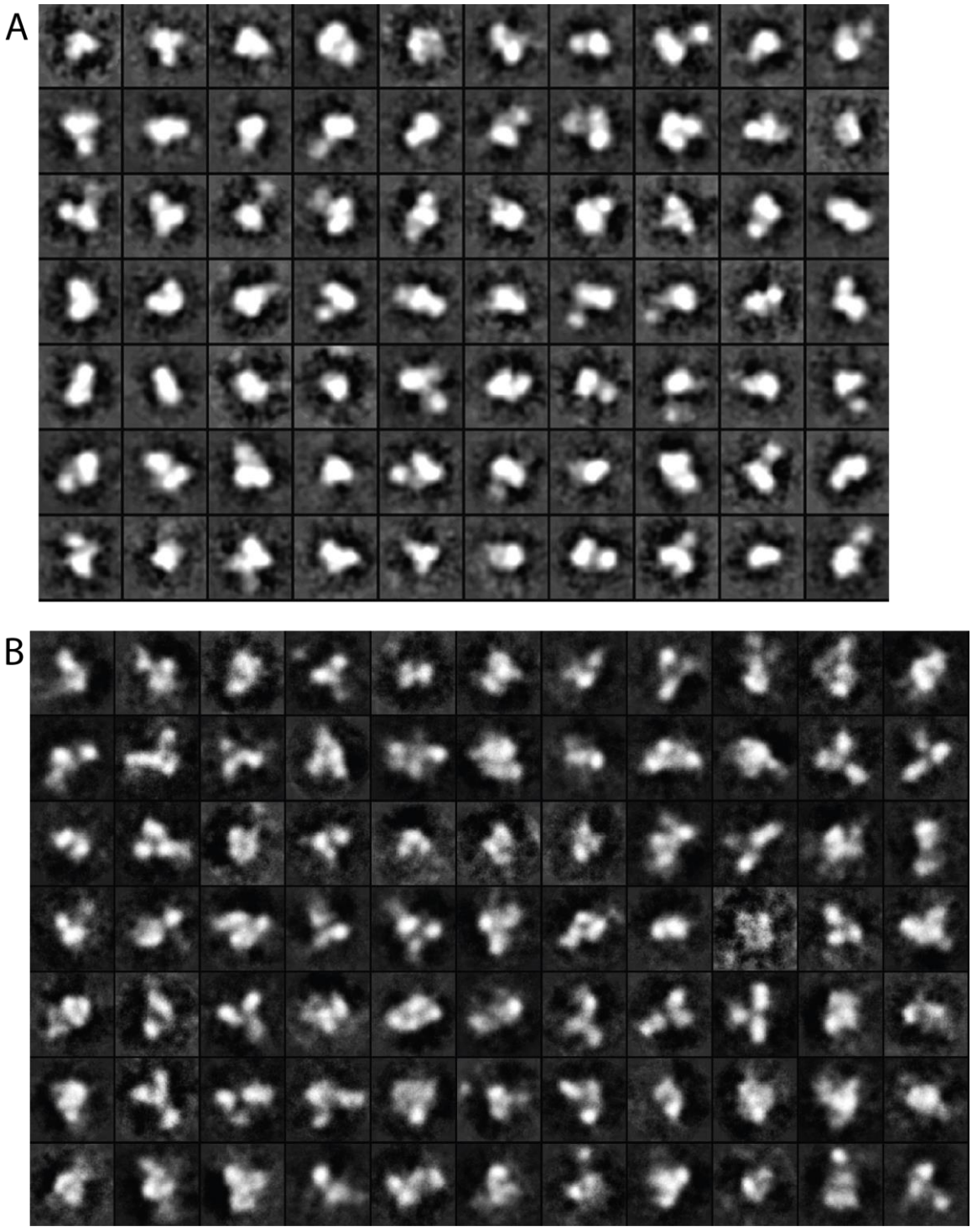

Figure S4: A) 2D classification of cyclically permuted gp120 trimers: 3,682 negative stained gp120 particle projections classified into 70 classes. B) 2D classification of cyclically permuted gp120 complexed with PGDM1400: 4,586 negative stained gp120 with PGDM1400 particle projections classified into 77 classes.

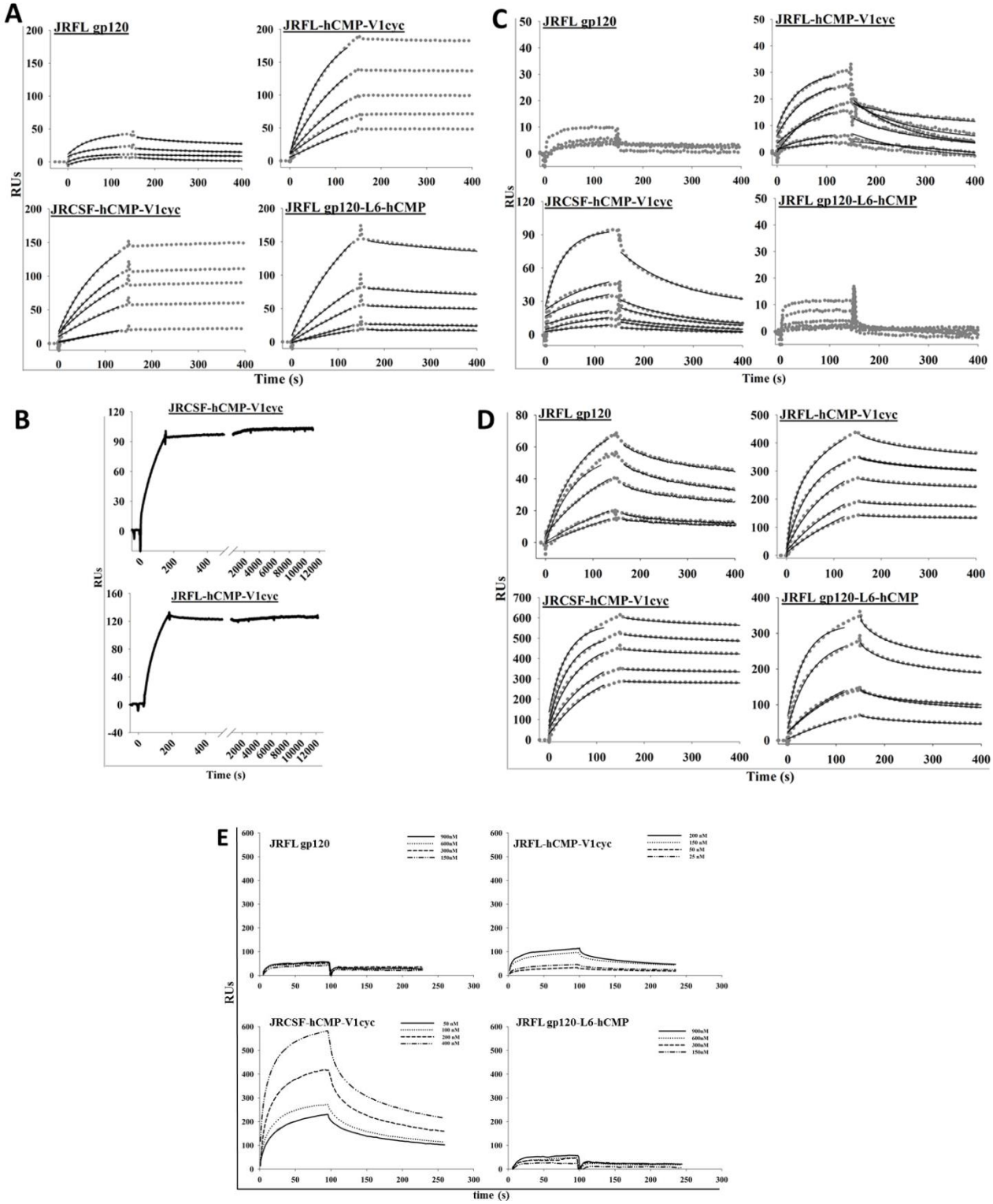
A
JRFL gp120
JRFL-hCMP-V1cyc
JRCSF-hCMP-V1cyc
JRFL gp120-L6-hCMP
RUs
Time (s)
B
JRCSF-hCMP-V1cyc
JRFL-hCMP-V1cyc
RUs
Time (s)
C
JRFL gp120
JRFL-hCMP-V1cyc
JRCSF-hCMP-V1cyc
JRFL gp120-L6-hCMP
RUs
Time (s)
D
JRFL gp120
JRFL-hCMP-V1cyc
JRCSF-hCMP-V1cyc
JRFL gp120-L6-hCMP
RUs
Time (s)
E
JRFL gp120
JRFL-hCMP-V1cyc
JRCSF-hCMP-V1cyc
JRFL gp120-L6-hCMP
RUs
time (s)

Figure S5: Cyclically permuted gp120 trimers display high affinity to various broadly neutralizing antibodies specific to different regions of gp120. Biacore sensogram overlays for binding of different immunogens to surface immobilized IgGs are shown. ~1000 RUs of each IgG were immobilized on individual CM5 sensor chips. In panel A, C and D, identical analyte concentrations of the four analytes were used ranging from 50-800nM going from bottom to top. In panel E, various concentrations of the four analytes were used ranging from 25-900nM. The kinetic parameters obtained after fitting the data to a 1:1 Langmuir model or double exponential decay equation are given in Table 1. A) Cyclically permuted gp120 trimers bind to CD4 binding site specific bNAb, VRC01 with higher affinities and lower dissociation rates than monomeric gp120. Due to undetectable dissociation of JRFL-hCMP-V1cyc and JRCSF-hCMP-V1cyc, the K_D values are not calculated and only association rate constants are given in the kinetic parameters table (Table 1). B) The cyclically permuted gp120 trimers do not dissociate from VRC01 immobilized surface even after extended dissociation times. Biacore sensogram traces for binding of 200nM each of JRFL-hCMP-V1cyc and JRCSF-hCMP-V1cyc to surface immobilized IgG-VRC01 are shown. The dissociation of these proteins from the VRC01 surface was monitored for ~200 minutes to determine the dissociation rates. No dissociation of cyclically permuted gp120 trimers from VRC01 was detected even after extended dissociation time. C) Cyclically permuted gp120 trimers bind to trimer specific bNAb, PGT145. JRFL-hCMP-V1cyc and JRCSF-hCMP-V1cyc bind to PGT145 while JRFL gp120 and JRFLgp120-L6-hCMP immunogens do not bind. D) Cyclically permuted gp120 trimers bind to V3 glycan specific bNAb, PGT128 with high affinity. JRFL-hCMP-V1cyc and JRCSF-hCMP-V1cyc showed higher association rates and lower dissociation rates with PGT128 relative to JRFL gp120 and JRFLgp120-L6-hCMP. E) Cyclically permuted gp120 trimers bind to quaternary epitope specific antibody bNAb PGDM-1400. JRFL-hCMP-V1cyc and JRCSF-hCMP-V1cyc bind to PGDM1400 in agreement with the negative stained EM data, while JRFL gp120 and JRFLgp120-L6-hCMP constructs do not show binding.

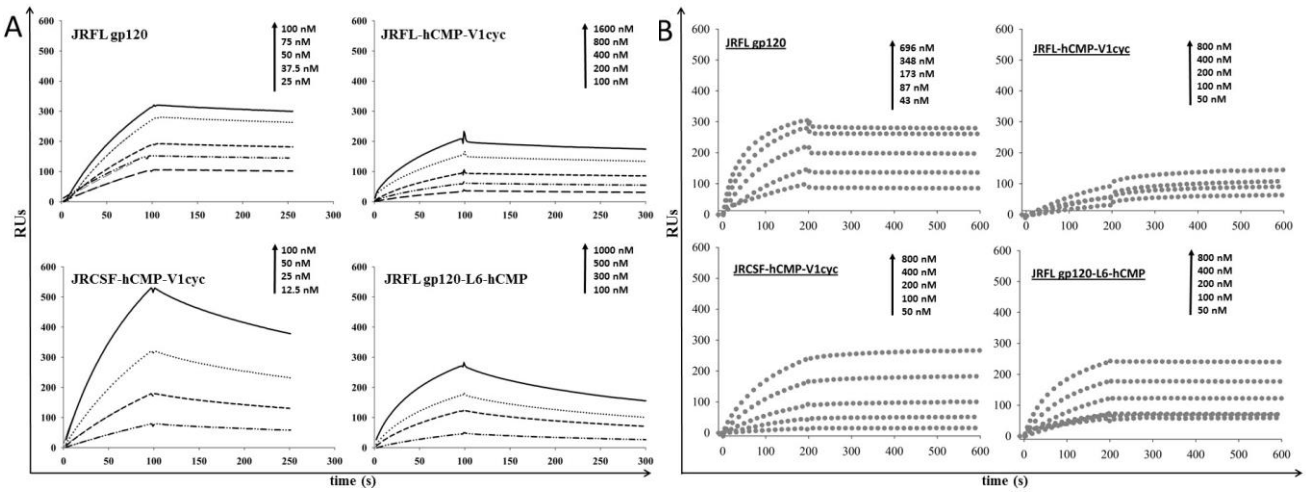

Fig S6: Cyclically permuted gp120 trimers did not show high affinities to CD4 binding site non-neutralizing antibodies F105 and b6 over bNAb VRC01. Biacore sensogram overlays for binding of different immunogens to surface immobilized non-neutralizing IgGs F105 and b6 are shown. In all cases, surface density was ~1000 RUs, buffer PBS (pH 7.4) P20, flow rate 30 µl/min, temperature 25°C. A) Binding of immunogens to F105 antibody was monitored over concentrations ranging from 12.5-1600 nM (from bottom to top). B) Binding of immunogens to b6 antibody was monitored over concentrations ranging from 43-800 nM (from bottom to top). The kinetic parameters obtained after fitting the data to a 1:1 Langmuir model are listed in Table 1.

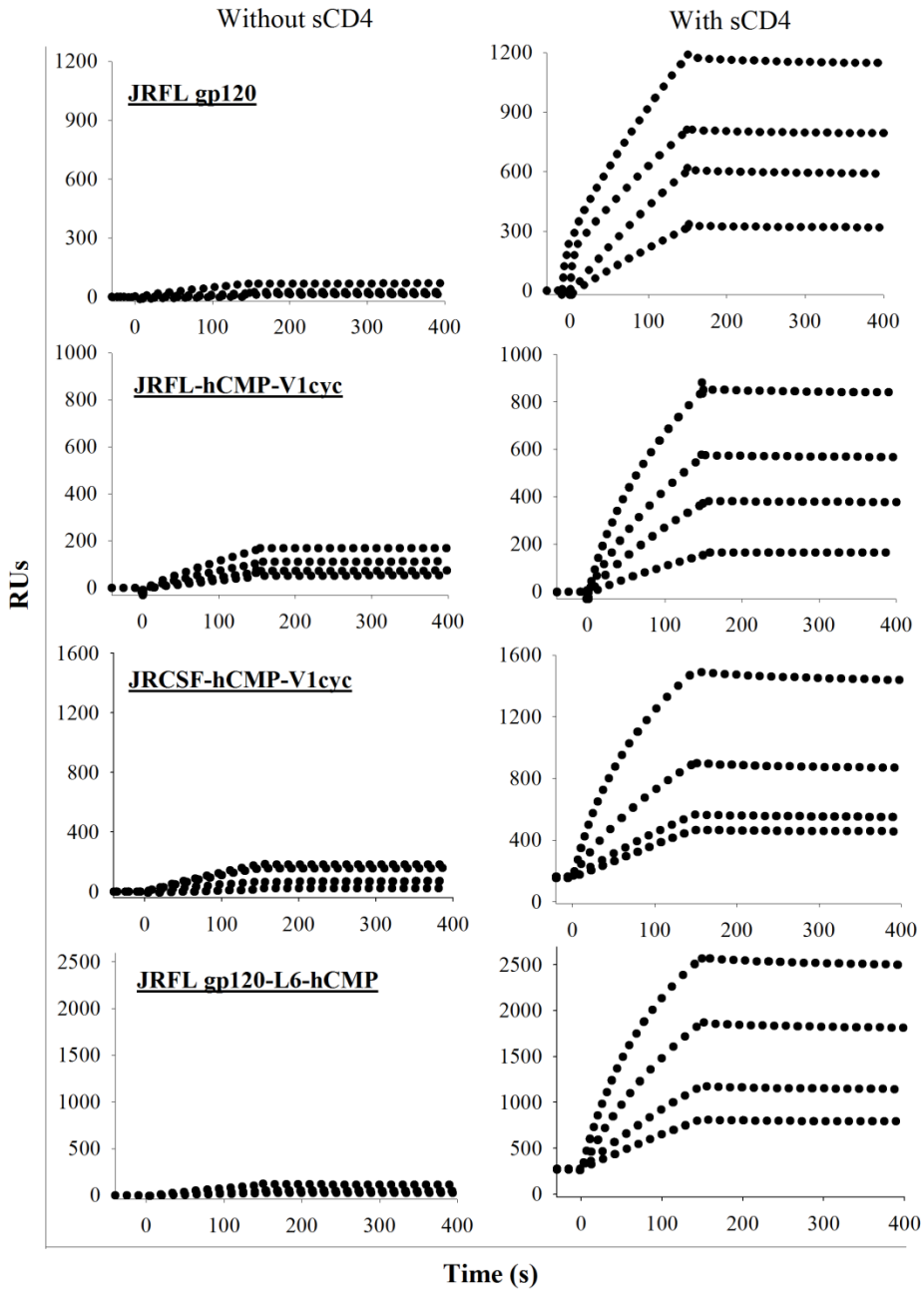

Figure S7: Cyclically permuted gp120 trimers bind tightly to CD4 induced epitopes in the presence of sCD4. Biacore sensogram overlays for binding of different immunogens to surface immobilized IgG-17b are shown. ~1000 RUs of IgG-17b were immobilized on a CM5 chip. Binding of various immunogens to 17b antibody was monitored over a range of concentrations (50nM to 400nM) in the absence (left) and presence (right) of sCD4. All immunogens showed low but detectable binding to 17b antibody in the absence of sCD4 and high binding in the presence of sCD4.

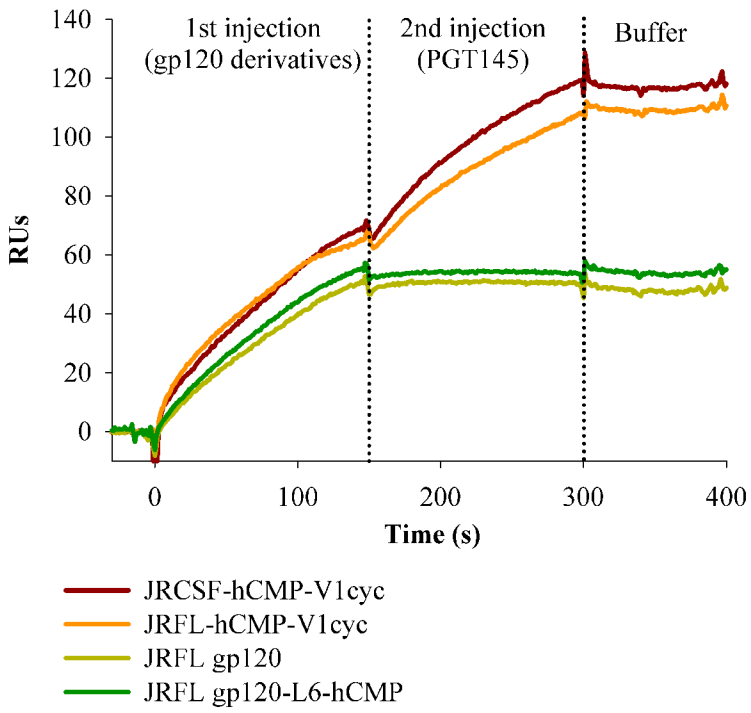

Figure S8: Binding of VRC01 antibody to cyclically permuted gp120 trimers stabilized quaternary interactions in gp120 trimers. Biacore sensogram overlays for sequential binding of different immunogens and PGT145 antibody to surface immobilized VRC01 antibody. VRC01 antibody was immobilized on a CM5 sensor chip and sequential injection of different immunogens followed by PGT145 antibody was carried out. These experiments suggest that cyclically permuted gp120 trimers retained binding to quaternary epitope specific antibody PGT145 even after VRC01 interaction.

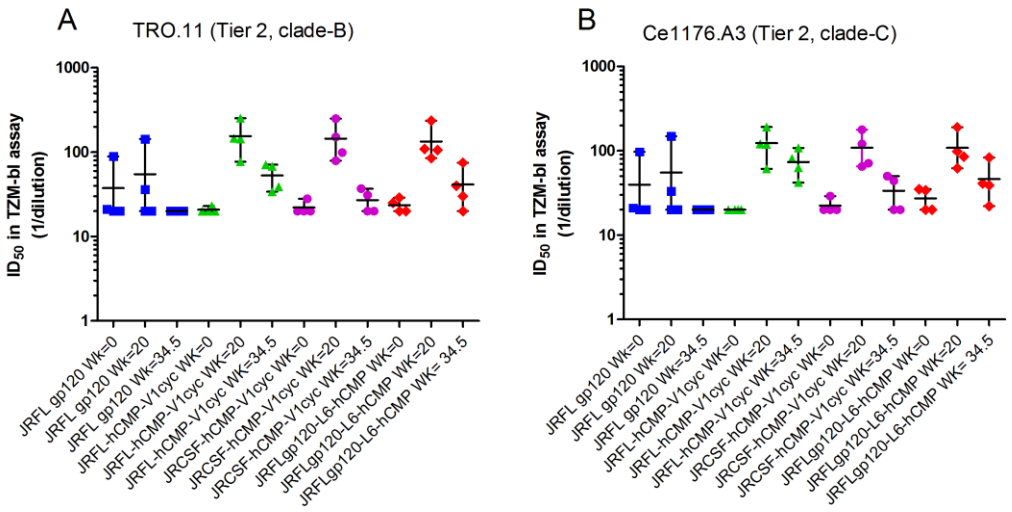

Figure S9: Neutralizing activity of week 34.5 (terminal bleed) sera for Tier 2 viruses from clade B and clade C (TRO.11 and Ce1176). Week 34.5 sera show detectable neutralization to Tier 2 viruses though the titers were 2-3 fold lower than the corresponding week 20 titers.

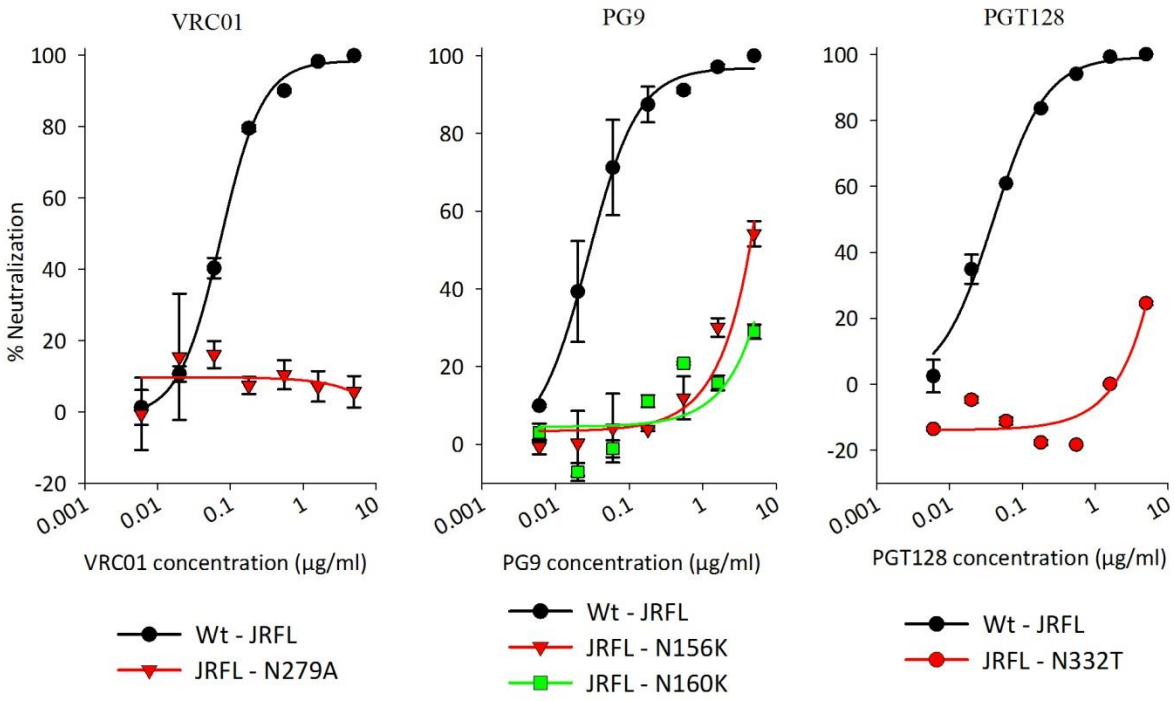

Figure S10: Neutralizing activity of VRC01, PG9 and PGT128 antibodies against wt-JRFL and JRFL Env mutant pseudoviruses in a TZM-bl assay. N279A mutation in Env abolishes the neutralizing activity of VRC01. N156K and N160K mutations in Env abolish neutralizing activity of PG9 or PG16 like NAbs. N332T mutation in Env substantially reduces the neutralizing activity of PGT128. To map the neutralizing specificities present in antisera elicited by cyclically permuted gp120 trimers, N279A, N156K, N160K and N332T mutations were introduced into JRFL Env, pseudoviruses were made and TZM-bl assays were conducted with VRC01, PG9 and PGT128 bNAbs for monitoring neutralizing activity.

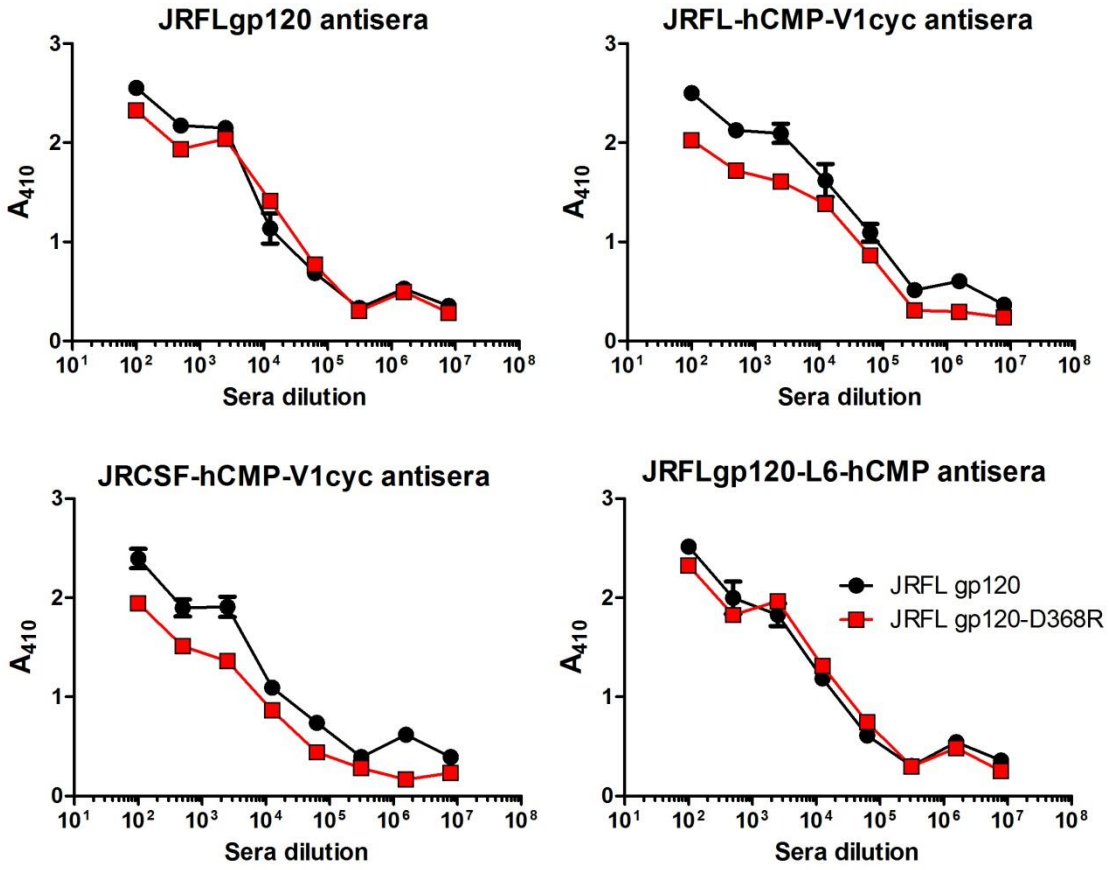

Figure S11: Binding of pooled antisera to JRFL gp120 and JRFL gp120-D368R. Antigens were coated directly onto ELISA plate wells and probed with pooled antisera from week 20. The absorbance at 410 nm (binding) was plotted as a function of antiserum dilution. Antisera from cyclically permuted gp120 trimers show marginally lower binding to the CD4 binding site mutant, JRFL gp120-D368R, than antisera from JRFL gp20 and JRFLgp120-L6-hCMP.

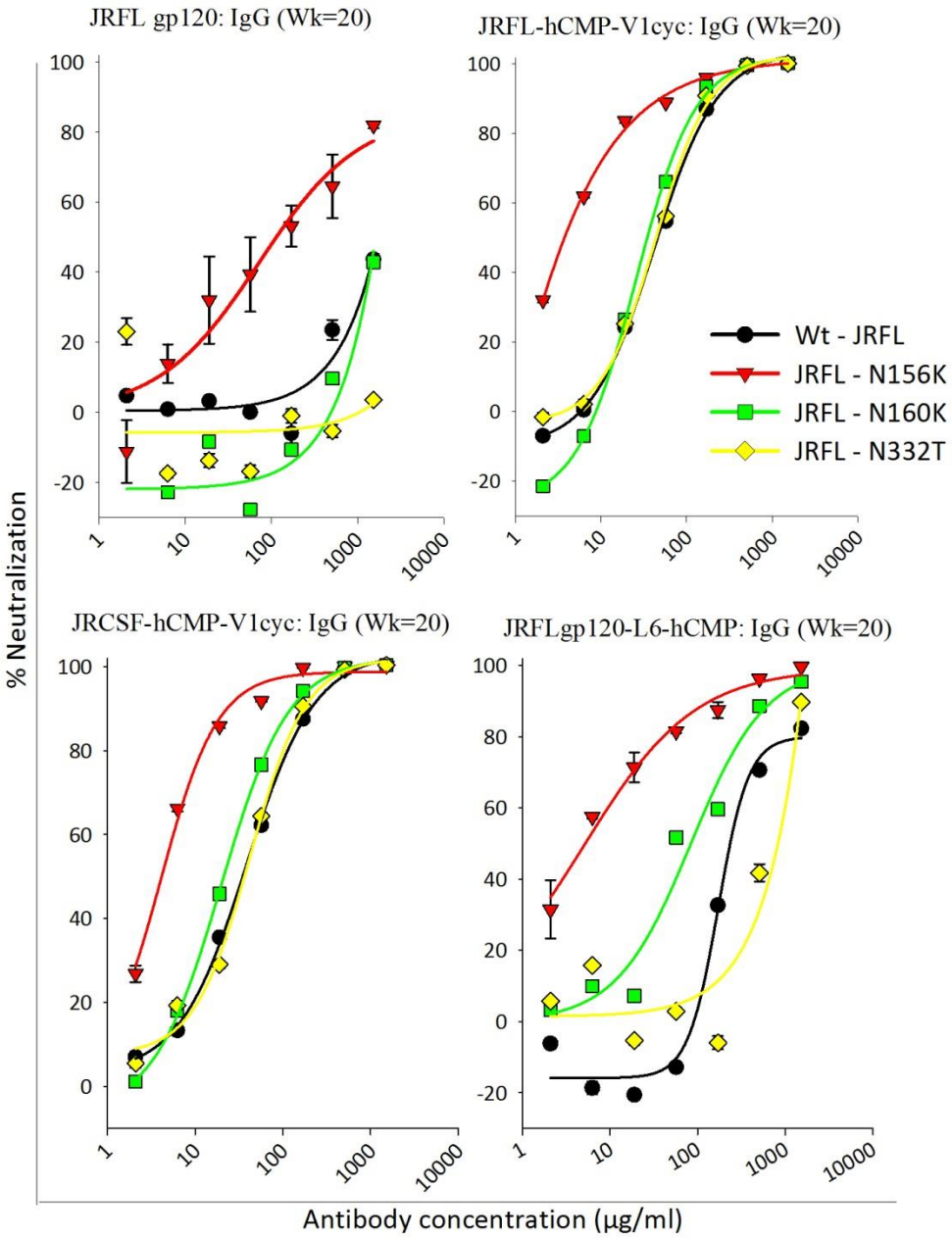

Figure S12: Neutralizing activity of IgG purified from pooled week 20 sera against wt-JRFL, JRFL-N156K, JRFL-N160K and JRFL-N332T pseudoviruses. Introduction of N156K or N160K mutation in Env makes JRFL pseudovirus resistant to neutralization by glycan dependent, V1V2 quaternary epitope specific Nabs (1) and N332T mutation makes JRFL pseudovirus resistant to neutralization by V3 loop glycan specific Nabs (2). Error bars represent the standard deviation from two independent experiments. Neutralizing activity of IgG from antisera of cyclically permuted gp120 trimers was not altered in the presence of N160K and N332T mutations. Increased neutralizing activity was observed when the N156K mutation was introduced in JRFL pseudoviruses.

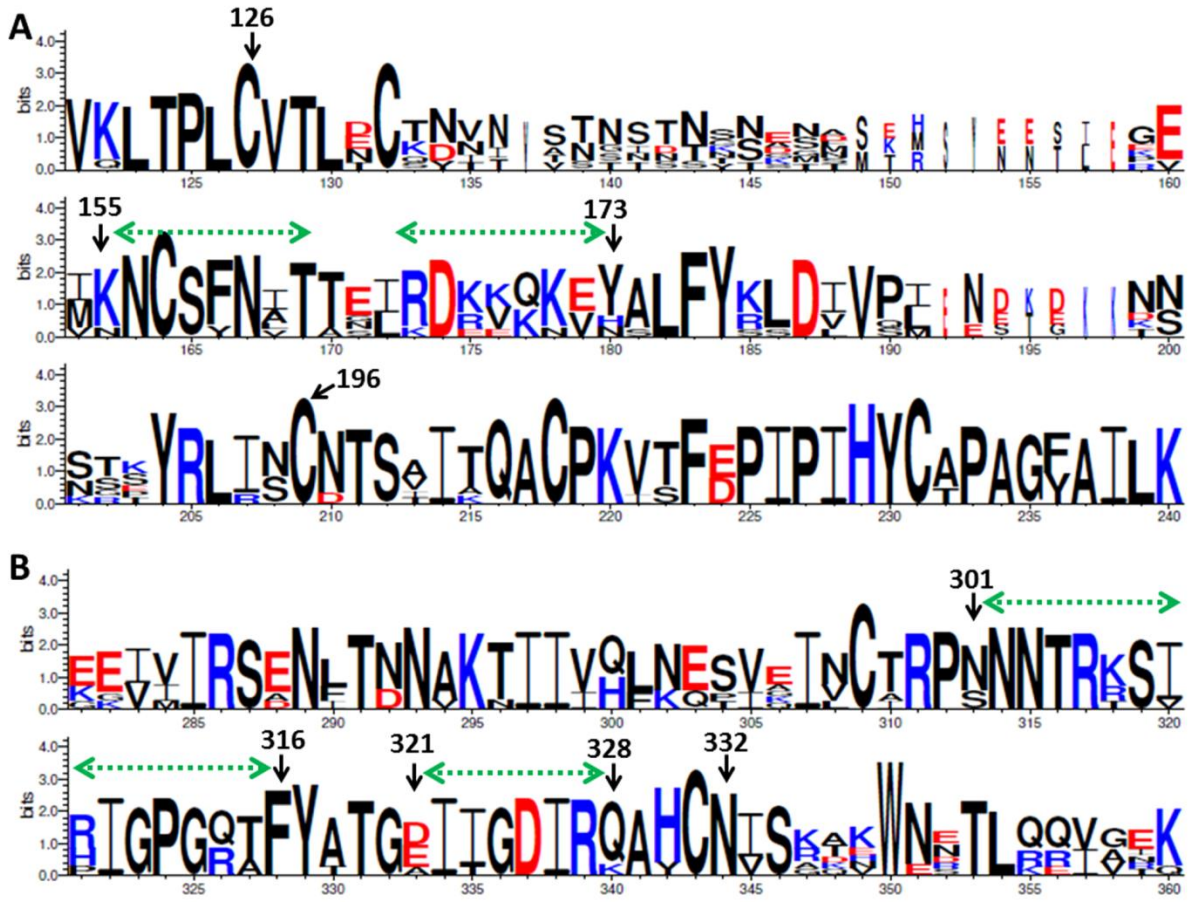

Figure S13: Conserved linear epitopes in the V2 and V3 regions of gp120. Multiple sequence alignment of gp120 amino acids of Tier-2 HIV-1 isolates used for neutralization assays. Multiple alignment of amino acid sequences was generated by Weblogo 3 server (http://weblogo.threeplusone.com/create.cgi). The height of an amino acid represents its level of conservation at that particular position. The amino acids marked in red are negatively charged residues and in blue are positively charged residues. A) The residue conservation at each position in the region V1V2 (residues 126-196) of gp120 is represented and the conserved linear epitope in the V2 region is indicated with a dotted green arrow. B) The residue conservation at each position in the V3 region (residues 301-332) of gp120 is represented and the conserved linear epitopes are indicated with a dotted green arrow. These conserved epitopes in the V2 and V3 region are surface accessible and immunodominant in nature (3-5).

References:

1. Doores, K. J., and Burton, D. R. (2010) Variable loop glycan dependency of the broad and potent HIV-1-neutralizing antibodies PG9 and PG16 *J. Virol.* **84**, 10510-10521
2. Walker, L. M., Huber, M., Doores, K. J., Falkowska, E., Pejchal, R., Julien, J. P., Wang, S. K., Ramos, A., Chan-Hui, P. Y., Moyle, M., Mitcham, J. L., Hammond, P. W., Olsen, O. A., Phung, P., Fling, S., Wong, C. H., Phogat, S., Wrin, T., Simek, M. D., Koff, W. C., Wilson, I. A., Burton, D. R., and Poignard, P. (2011) Broad neutralization coverage of HIV by multiple highly potent antibodies *Nature* **477**, 466-470
3. Nicely, N. I., Wiehe, K., Kepler, T. B., Jaeger, F. H., Dennison, S. M., Rerks-Ngarm, S., Nitayaphan, S., Pitisuttithum, P., Kaewkungwal, J., Robb, M. L., O'Connell, R. J., Michael, N. L., Kim, J. H., Liao, H. X., Munir Alam, S., Hwang, K. K., Bonsignori, M., and Haynes, B. F. (2015) Structural analysis of the unmutated ancestor of the HIV-1 envelope V2 region antibody CH58 isolated from an RV144 vaccine efficacy trial vaccinee *EBioMedicine* .**2**, 713-722
4. Gorny, M. K., Revesz, K., Williams, C., Volsky, B., Louder, M. K., Anyangwe, C. A., Krachmarov, C., Kayman, S. C., Pinter, A., Nadas, A., Nyambi, P. N., Mascola, J. R., and Zolla-Pazner, S. (2004) The v3 loop is accessible on the surface of most human immunodeficiency virus type 1 primary isolates and serves as a neutralization epitope *J. Virol.* **78**, 2394-2404
5. Hioe, C. E., Wrin, T., Seaman, M. S., Yu, X., Wood, B., Self, S., Williams, C., Gorny, M. K., and Zolla-Pazner, S. (2010) Anti-V3 monoclonal antibodies display broad neutralizing activities against multiple HIV-1 subtypes *PLoS One* **5**, e10254